Acoustic Detection of Pad Craters in Mechanical Shock and Transient Bend Tests

Julie Silk[1], W. Carter Ralph[2], Gregory Morscher[3], Elizabeth Benedetto[4], Douglas Olney[1]
[1]Keysight Technologies,[2]Southern Research Institute, [3]University of Akron, [4]HP Inc

Abstract
Printed circuit assemblies have become more susceptible to a failure mode known as "pad cratering" due to the implementation of several material restrictions. Pad cratering is defined as mechanically-induced fracture between the copper pad/trace and printed circuit board (PCB) laminate. If left undetected during manufacturing, pad cratering can significantly reduce the reliable life of electronic products. The industry needs a fast, precise, non-destructive method to assess pad cratering, as it increasingly moves toward thinner, more mobile products. There are several methods being used in the electronics industry, both destructive and non-destructive, but all have significant limitations. Acoustic emission detection is a broad-area, non-destructive technique that has the potential to detect solder joint fractures. Passive acoustic emission detection (AED) records the sound waves emitted by fracture events during structural loading. This technique typically employs an array of piezoelectric transducers to measure sound waves at the surface; the location of the fracture event is calculated using the positions of the sensors, the time delay between the arrival of the events at the sensors, and the sonic velocity through the medium. This article discusses the development work performed to date by the authors in both transient bend and shock. The general test and data analysis methods are discussed. Transient bend and shock tests, results, and validation are described. Finally, further potential for the application of these methods to the electronics industry IPC-9709 are presented.
Keywords: acoustic emission, printed circuit reliability

Introduction
With the use of stiffer SnAgCu solders and the more brittle printed circuit board (PCB) laminates capable of surviving the necessary higher reflow temperature, there has been an increase in the failure mode called pad cratering, Figure 1. This is a mechanically-induced cohesive failure of the laminate's outmost layer, typically under the pads of a ball grid array (BGA). The failure can occur during manufacturing processes that bend the PCB or during handling after manufacturing, such as shock/drop events. Pad craters are not electrically detectable until they propagate through the laminate and sever the connecting trace. Electrical failure can occur well after shipment, leading to dissatisfied customers. The electronics industry has been working on ways to detect and prevent this issue[1, 2].There is much work to be done on comparative robustness of laminates, and determining risk levels for specific components and assemblies. Most techniques require destructive and expensive analysis that inhibits extensive testing.

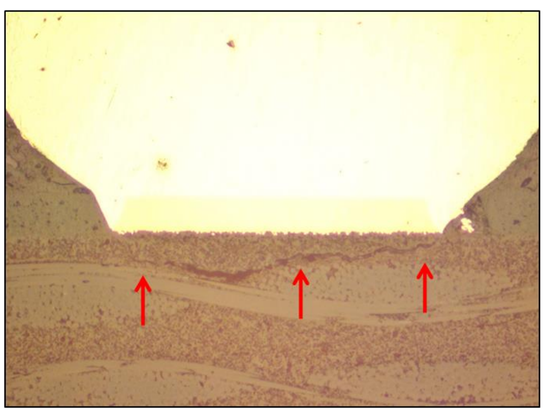

Figure1 - Pad crater under a BGA pad, as observed in a cross-section

Acoustic emission detection (AED) uses the sound waves emitted by the fracturing laminate to identify when and where failure occurs. This technique is used for identifying fractures in large structures and can be adapted for PCBs. Sound waves are measured at the surface of the PCB using piezoelectric transducers. The time delay to each of the sensors and sonic velocity through the PCB allows calculation of the fracture location. Initial work on this technique demonstrated viability and led to the creation of IPC-9709 Test Guidelines for Acoustic Emission Measurement During Mechanical Testing, an initial document describing tools and procedures to perform AED with transient bend. Additional work with transient bend testing and data analysis has been done [3,4,5]. In addition, AED has been used with mechanical shock testing [6,7], where the bend event is much faster, in the range of 10 milliseconds, versus transient bend, which is around 500 milliseconds. In mechanical shock, the acoustic events are much closer together and there is more acoustic noise from instrumentation and fixtures. The data analysis is therefore more critical to enable detection of the events of interest.

This development work is described here, with recommendations for applications of AED and proposals for updating IPC/JEDEC 9709, Test Guidelines for Acoustic Emission Measurement during Mechanical Testing.

Detection and Data Analysis Methods

The studies in this paper employed a modal acoustic emission detection system in which sets of acoustic waveforms are captured for each event. An example of a set of four waveforms for a single event is displayed in Figure 2. This shows that the event arrived at the four transducers within approximately twenty microseconds of each other and that the arrival time at each transducer is clearly evident, marked by the black arrow. The system continuously buffers the voltage signals from multiple transducers, monitors them for voltage triggers of a preset amplitude, and stores a preset amount of data for all the transducers before and after each trigger. If the location of each transducer and the sonic velocity through the PCB are known, the location of each event can be calculated from the arrival times.

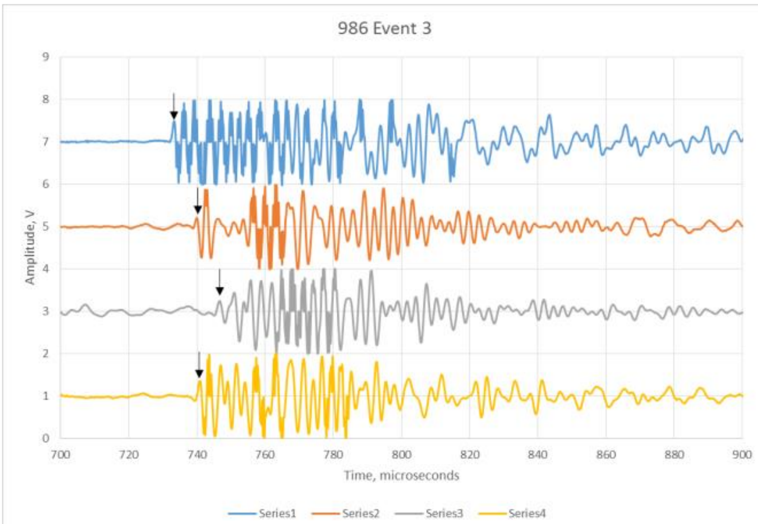

Figure2 - A set of waveforms for an event. Black arrow marks the arrival time at each transducer.

The acoustic emission tests employed the use of wide-band transducers that are sensitive to at least 100 and up to 700 kHz or higher with a flat frequency response. A sampling rate of 10 MHz or higher was used for all experiments. A 20dB preamplifier was used to amplify the signal. Better results were achieved by setting the amplification such that the waveform responses of interest were just at the point of saturation, then setting the trigger to be slightly above the noise generated by the test frame. In some tests, additional amplification is needed. An example of a transducer mounted to a PCB is shown in Figure 3. Vacuum grease was used as a coupling agent to enhance the sound wave into the sensor. Other couplants are petroleum jelly or other viscous materials. Transducers can be attached to the board with a mechanical clamp or cyanoacrylate; a thin layer of accelerometer wax, as shown in Figure 3, gave comparable results with easier application and removal, so was used in the majority of this testing.

Figure 3 - Acoustic transducer mounted to a PCB with accelerometer wax

For each test, pencil lead breaks (PLB) were used, per ASTM E976-15, to assess the ability of the transducers to record the sound waves. This also enabled the determination of speed of sound between different sets of transducers which was utilized in location analysis. The waveform time window was predetermined based on the type of test. Longer time windows (tens of milliseconds) were used for drop tests since so much AE activity was created associated with the test itself (stress waves are created when impact occurs) in addition to the microfractures associated with pad crater breaks. Shorter time windows (hundreds of microseconds) were used for the slower bend tests since independent discrete events occurred much further apart from one another in time without the risk of the computer "locking out" events the computer could not record while rearming for the next capture. Each waveform is digitized and stored which allows access for post-test analysis at a future time.

During post-test analysis, the raw data is processed to screen out acoustic events that are not of interest, and then the events of interest are analyzed to determine damage initiation. Data processing, typically automated by software, involved calculating the waveform energy and event location. The events were then screened by energy and location. Low energy events are difficult to locate due to their low signal-to-noise ratio, and were found to not correspond to solder interconnect damage, covered in the next section. Events that were located outside the boundary of surface mount components or at illogical locations (such as beyond the PCB edges) were considered not to be of interest. Parametric inputs from other test equipment, such as load cells and displacement gages, were often used to help synchronize the acoustic data with the test, and the time of the event could also be used to discard events that happened either too early or late in the test to be of interest. The events of interest could then be plotted in many informative ways by energy, time, location, load, displacement, strain, and acceleration.

The raw AED data from shock testing, as represented in Figure 4 over time, magnitude and frequency, is very noisy and complex. The acoustic events that correlated to pad cratering from shock/drop were manually selected in this study. Additional post-processing of this acoustic data, shown 2 dimensionally in Figure 5, has since been done to explore ways to systematically identify the events. Applying a 350 MHz high pass filter to the data, as shown in Figure 6, isolated the high frequency events of interest, but shifted the arrival time slightly. Further development of this technique may allow automated selection of relevant events.

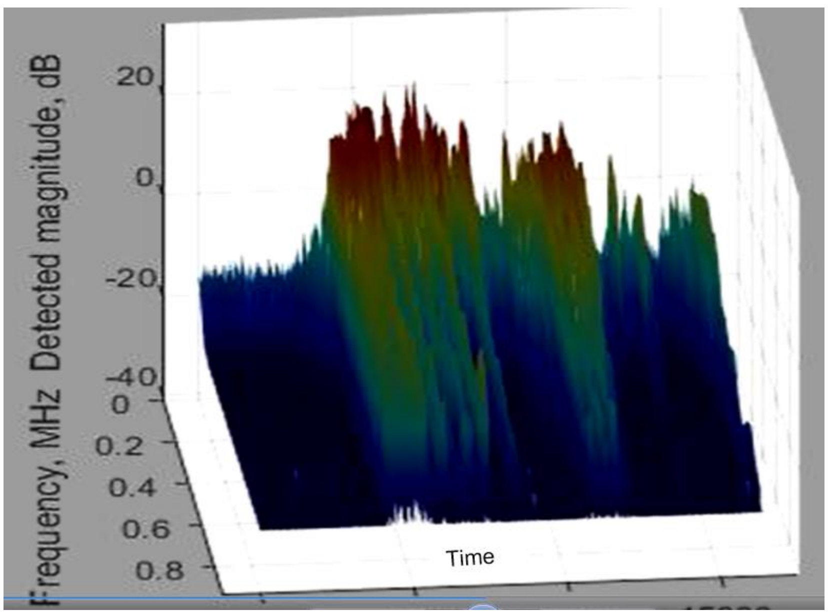

Figure 4 – 3D Representation of AED Data.

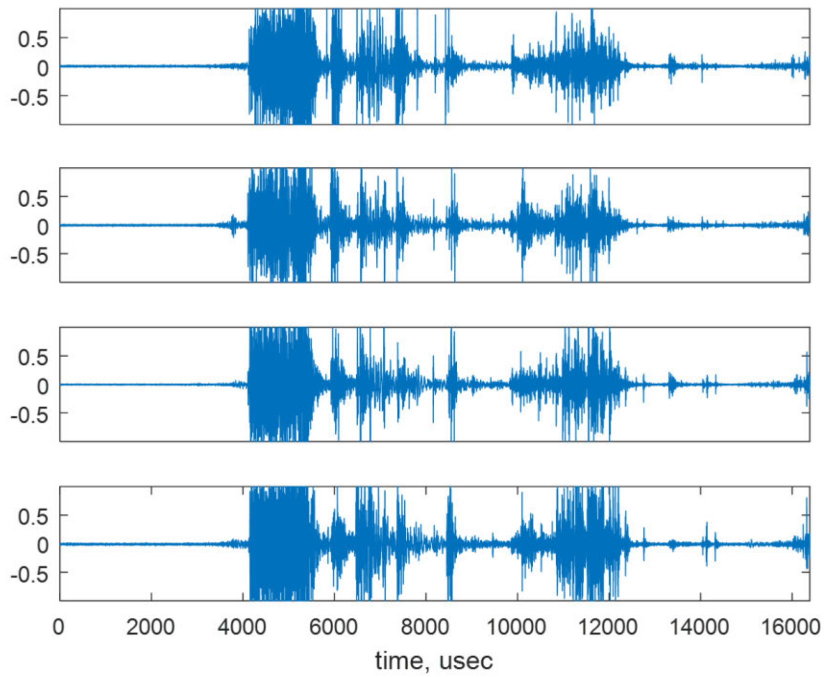

Figure 5 – Raw AED Data from Shock Testing

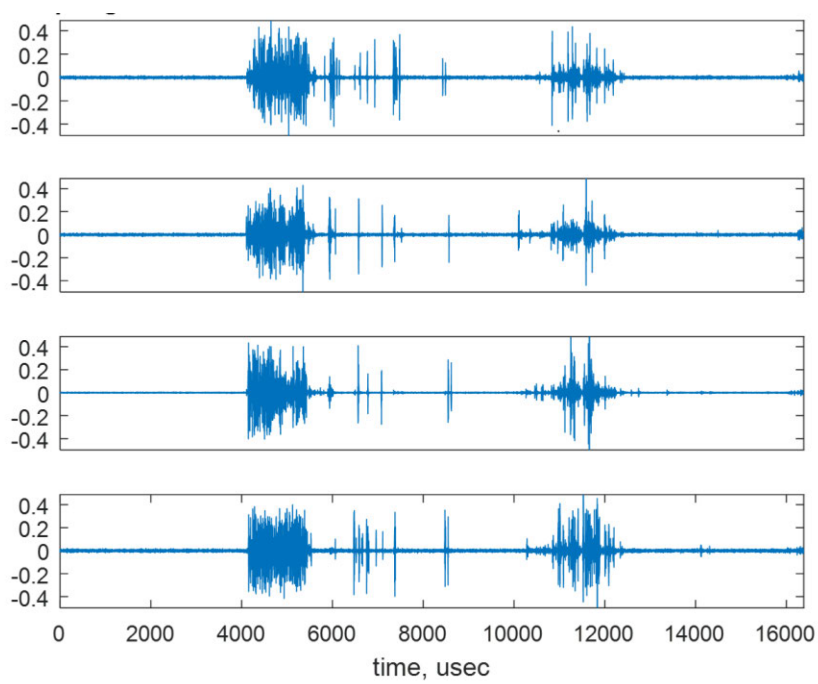

Figure 6 – AED Data after High Pass Filter

Flexure Test Method and Results

The initial studies [3] used an industry-standard test method commonly referred to as the spherical bend test and documented in IPC/JEDEC 9707. The goal of the test is to replicate the worst-case bending conditions of in-circuit test. The test can be thought of as a three-dimensional version of three-point bend, where the board rests on eight points with the component facing down in the center of the points, and a ninth point applies load to the other side of the board at the center of the component. The eight points are arrayed in a circle with a diameter that is three times the width of the component. A strain gage rosette is placed 5mm from each corner of the component to measure the relative strain conditions at the locations most likely to fail first. The test article, Figure 7, is a 160x160mm wide, 8 layer, 1.6mm thick FR4 PCA with a 35x35mm daisy-chained PBGA with 1mm solder ball pitch. This PCA was designed for the spherical bend test with eight flat features on the upper surface that match the locations of the eight supporting points and an array of pins at each corner that connect to the strain gage leads and daisy chains. The spherical bend test fixture is shown in Figure 8, along with a photograph of a test article mounted on the fixture ready to test. The aluminum angle brackets at the front left and back right corners of the PCA are alignment fixtures that are spaced a paper's width from each edge so that they do not make contact during the test. Four acoustic emission transducers were placed on each test article, typically 38mm from the center of the BGA along the diagonals (near the corners).

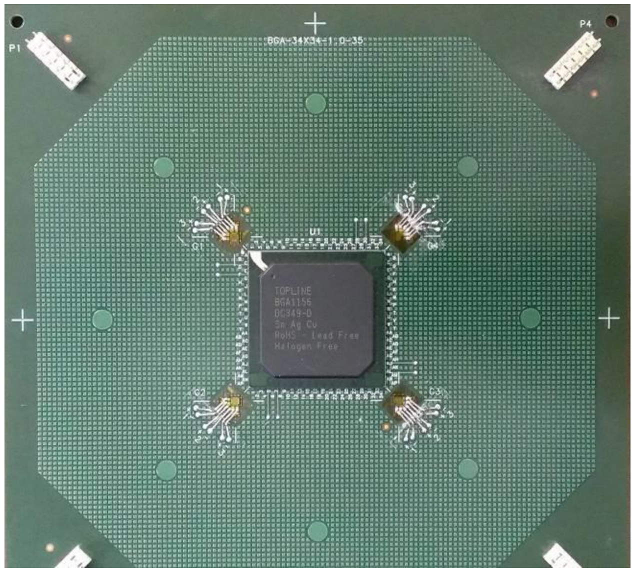

Figure 7 - Test specimen for spherical bend

Figure 8 - Spherical bend test fixture and setup

The initial tests were performed at a slow (quasi-static) displacement in a screw-driven test frame at a rate of 1mm/minute in order to allow the test to be stopped manually when damage was detected. This displacement rate produced approximately 700$\mu\varepsilon$/minute ($7x10^{-4}$ mm/mm-minute), compared to the recommended 5,000$\mu\varepsilon$/second in the test standard. Six test articles were initially tested at this rate, and all tests produced a similar trend of acoustic responses, which are shown Figure 9 and roughly divided into three stages. In this figure, the relative magnitude of each acoustic event is summed to show the running total in order to make the trend easier to visualize. The first stage consisted of an initial period of no acoustic response followed by an onset of low magnitude events. In the second stage the low magnitude events continue, but at a noticeably lower rate. In the third stage the magnitude of the events suddenly increase by 2-3 orders of magnitude and remain relatively large until the PBGA visibly begins to separate from the PCA. The location of origin of each acoustic event was calculated from the locations of the transducers, the sonic velocity of the PCA (measured with pre-test pencil lead breaks), and the difference in acoustic event arrival times between the four transducers. The acoustic emission results are plotted by location, magnitude, and time in Figure 10, showing the scattered and early low magnitude events and the high energy events initiating near the PBGA corners. These test articles were inspected for damage using both dye stain and cross section, and pad craters were identified in damaged parts. The acoustic events produced in Stages 1 and 2 were scattered throughout the PCA, while the events in Stage 3 were located within the perimeter of the PBGA. Both the pad craters and the initial Stage 3 acoustic events were consistently concentrated near the corners of the PBGAs. The events in Stages 1 and 2 were attributed to small-scale damage in the PCA, such as fiber-matrix debonding, while the high magnitude events in Stage 3 were attributed to pad craters.

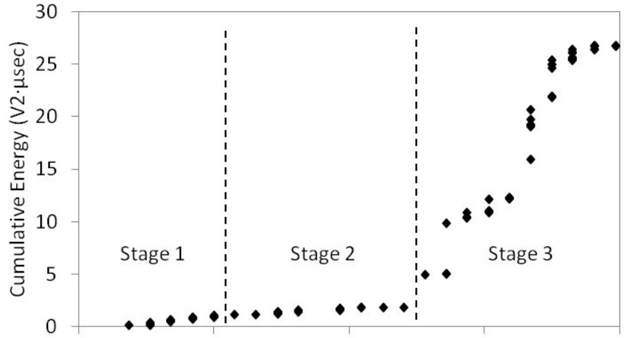

Figure 9 - Typical cumulative energy plot showing three stages of acoustic activity

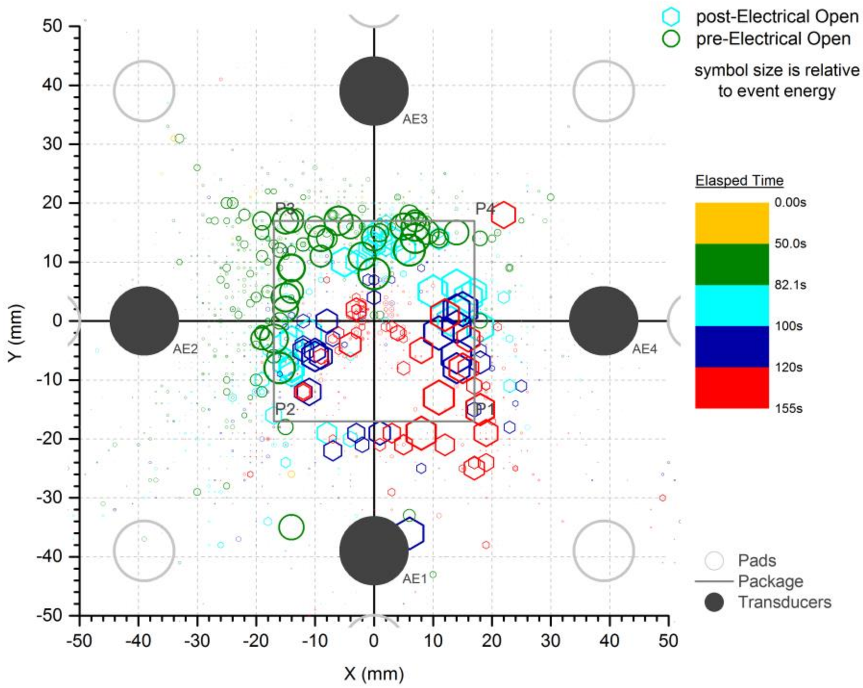

Figure 10 – Acoustic Event Progression

Once the acoustic trend was established, two test articles were first bent to either 400, 500, 600, or 700µε and inspected with dye penetrant. Pad craters were only observed in one test article, which was bent to 700µε and was the only test that produced high-magnitude acoustic events. The pad craters were from the same corner from which the acoustic events originated. Three additional test articles were then bent until two high energy events were detected. Dye staining revealed between 4 and 29 pad craters in the corners of each BGA. It is interesting to note that the number of pad craters in the higher displacement tests exceeded the number of acoustic events, suggesting that each release of energy stored up during the bending of the PCA can cause several pad craters before the damage arrests.

A third round of testing was performed in order to determine whether the same trends are observed at the higher bending rates and to attempt to demonstrate more definitively that the high magnitude acoustic events are caused by pad craters. The tests were performed in a servo-hydraulic test frame in displacement control at a rate that produced approximately 5000µε/second. The test articles were bent to progressively higher displacements, starting at levels expected to be just below the Stage 3 threshold, until high-magnitude events were definitively detected. The first three tests were performed to 0.89, 1.02, and 1.14 mm with no high-magnitude events. The fourth test, bent to 1.27mm, produced a two high-magnitude events, so the displacement for the fifth test was increased again to 1.40mm and produced several high-magnitude events. The displacement was reduced back to 1.27mm for the final test, which also produced several high-magnitude events. The magnitude versus time plot for these six tests are shown in Figure 11. No damage was detected in any articles bent to the lower displacements, but 2, 53, and 5 partial pad craters, respectively, were observed in the articles bent to the higher displacements. The failure analysis results from the fourth test are particularly informative, and are shown in Figure 12. Only two partial pad craters were detected in that BGA, both from the same corner as the two acoustic events, giving confidence to the conclusion that these high magnitude events are pad craters.

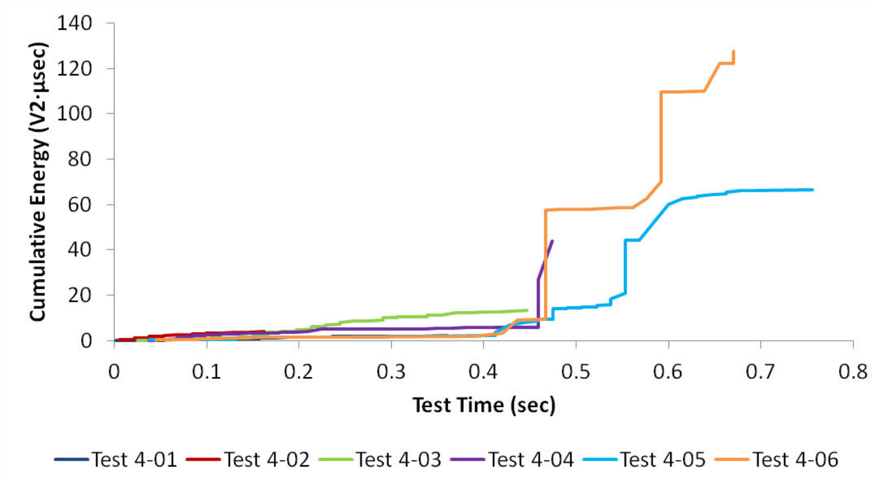

Figure 11 – Cumulative Magnitude versus Time for High Rate Tests

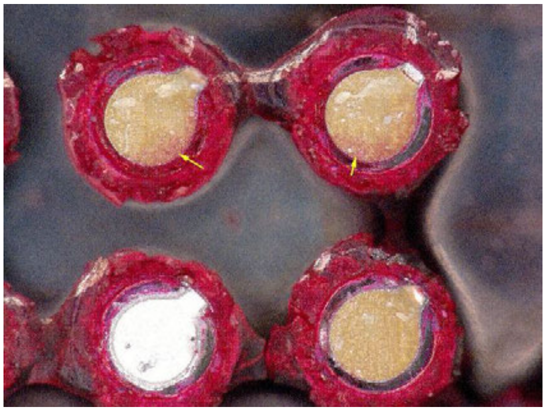

Figure 12 - Dye stain (left) on the fourth PCA from the high rate test showing pad cratering

Shock Test Method and Results

The current IPC-9709 document covers only flexure testing. Pad cratering is known to occur in mechanical shock testing, such as when a product is dropped. To attempt to expand the AED method, the same tactics used on flexure testing were adapted to mechanical shock [6,7]. There are significant differences because a single mechanical shock leads to multiple bend events in the board, and tying any one event to failure analysis results is difficult. The test is also at higher speed, so the acoustic events are much closer together, with more noise from fixtures, instrumentation and reflections. It can be difficult to detect interconnect damage. Therefore, long time windows are captured and isolated AE events must be sorted out manually within the long-time capture window according to their times of arrival on each channel based on the speed of sound of the board. For example, those events in Figure 6 between approximately 6000 and 9000 seconds were examined to determine which events had times of arrivals within a few microseconds of one another (the initial dense region of AE between 4000 and 5500 seconds was the sound of initial impact of the entire structure prior to flexure of the board). If the times of arrival were greater than this, then these events were deemed to have originated in an area outside the area of interest (e.g., at one of the mounting points of the board to the drop-tester base). Work is underway to be able to sort out these events digitally.

The test vehicle used in this work was a 35x35 mm PBGA package with 1 mm pitch SAC305 solder balls with non-solder mask defined pads on a 1.6 mm thick, 203x203 mm board, shown in Figure13.Transducers can become dislodged during even flexure testing; with shock tests, this was even more likely. Smaller transducers with 9mm diameter were used to reduce dislodgment. The transducer wires were attached near the transducer body with putty and taped to the board to prevent slapping against the board and generating additional acoustic noise. The amount of input energy was measured with an accelerometer on the shock table. The sampling rate was 5 MHz, and either 16384 or 8192 acoustic waveform data points were saved post-trigger, while 1638 points were saved pre-trigger. A 50 kHz high pass hardware filter was set on the signal, and a 1.5 MHz low pass filter was set on the trigger.

The overall pre-amp was typically set at 24 dB; the recorded signal was amplified 18 dB; and the trigger was amplified 6 dB. A level of 100g was found to be below the damage threshold; a level of 150 to 200g was used to induce pad craters. See Table 1.

Table 1 - Preliminary Shock Test Results

Shock Level (g)	Dye Stain Results
100	No opens
150	No opens
250	2 partial cracks
350	Partial and full cracks across component
400	Full opens across most of component

During the subsequent testing, if no acoustic signals were detected, the boards were dropped additional times. After the tests, select boards were analyzed with dye stain or cross-sectional analysis to compare results, shown in Table 2. It was found that dye stain did not always detect pad craters – if the fracture did not reach the surface, dye did not penetrate. For example, the AED data showed a possible crack on board 1A027, but dye staining did not show this. Cross-sectional analysis gave better correlation with AED results and was used on the majority of boards.

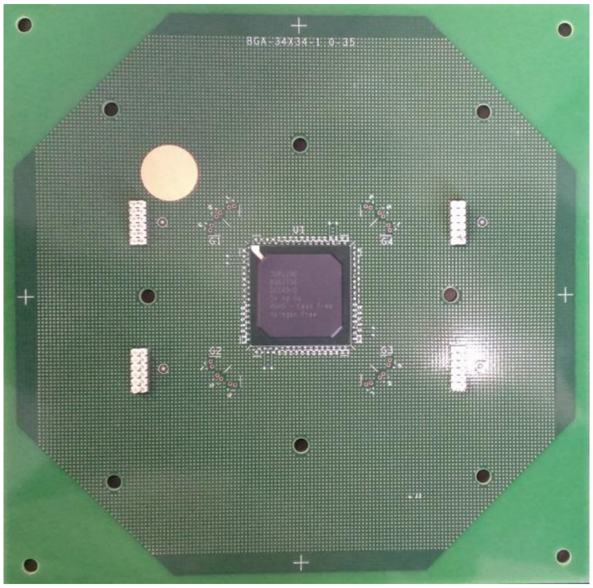

Figure 13 - Shock Test Vehicle

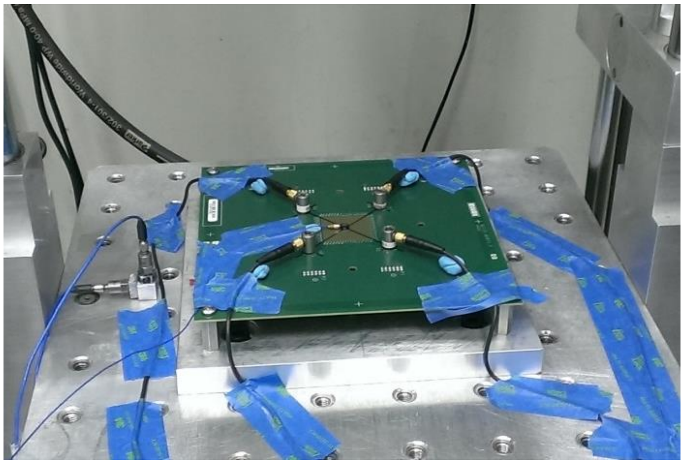

Figure 14 - Test Article Setup

Table 2 - Shock Tests with Acoustic and Failure Analysis Results

Board	Drop Inputs	FA Results	Acoustic Events
Z986	1 @ 250g	Dye stain: 3 partials at corner 1	High amplitude event near corner 1
Z988	8 @ 130g	Dye stain: no opens found	Several high amplitude events around corner 2
Z990	1 @ 175g	Dye stain: sensor 3 one partial	Only one high amplitude event on near 2 and lower amplitude events near 3
Z991	5 @ 150g	Dye stain: no opens found	One high amplitude event at 3
Z992	5 @ 150 to 225g	Dye stain: 1 partial sensor 1 and 2 partials sensor 3	Multiple high amplitude events near sensors 1 and 3 and a single event near sensor 2
Z997	10 @ 100g	Dye stain: no opens found	No high amplitude events
1A027	1 @ 200g	Dye stain: no opens found	High amplitude event near corners 1 and 2, medium event near 1
1A030	1 @ 200g	Dye stain: partial open at corner 3	Medium amplitude events near corners 2 and 3
Z976	1 @ 225g	Cross section: partial cracks at corners 1 and 3, die cracking	Several high amplitude events at 1 and two moderate events at 4
D160	2 @ 175g	Cross section: partial cracks at all corners, with multiple partials at 3	One medium amplitude event near 4 and one near 3
E175	1 @ 125g	Cross section: partial crack at corner 3	One medium amplitude event near 3 and one near 1

Dye stain did not always confirm the AED events, Figure 15; we suspect that the events did not fracture to the PCB surface, so that dye could not penetrate. In each case where AED indicated a fracture within 5 mm of the corner of a ball grid array package, cross-sectioning confirmed the pad crater. This indicates that AED can successfully be used to detect pad cratering in shock testing, often with enough sensitivity to detect these at the crack initiation phase.

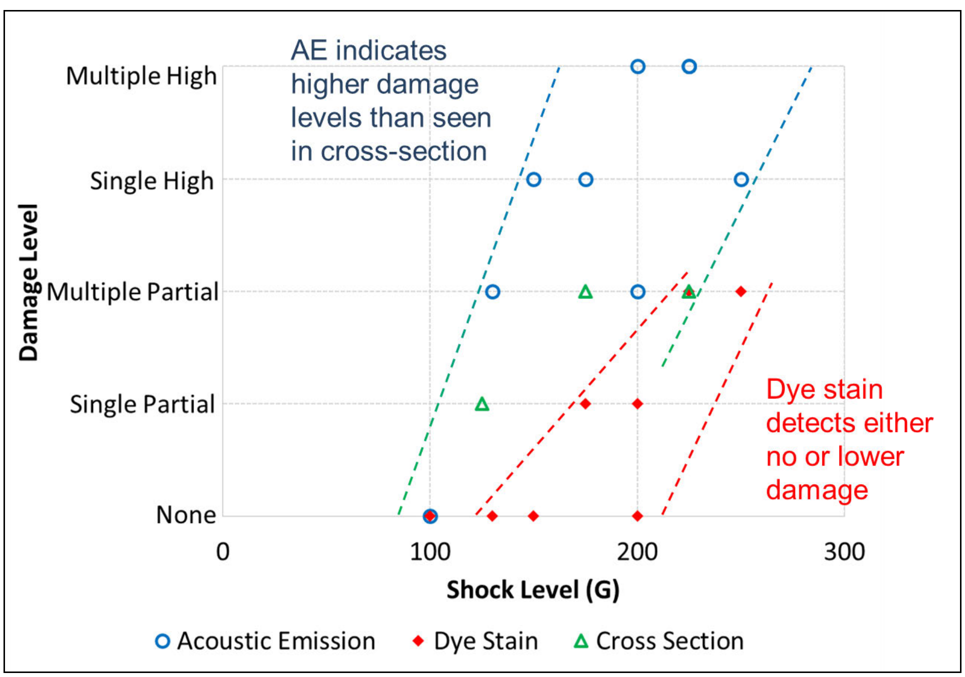

Figure 15 – A Comparison of AE Damage Detection to Failure Analysis Results

Further Development Potential

Additional development can be done to improve the method. The acoustic emission system used required re-arming, and could not collect data during this time; the use of a digital oscilloscope may improve this. Data processing techniques could be enhanced to detect relevant events systematically. When enough confidence is gained in AED, the number of cross-sections performed for confirmation of failure could dramatically decrease.

To help the industry incorporate the best test practices and data analysis discussed in the prior sections, there is an opportunity to improve upon the existing industry standard. IPC-9709, Test Guidelines for Acoustic Emission Measurement during Mechanical Testing, currently outlines how to utilize acoustic emission testing to detect printed circuit assembly pad craters in 3-point bend. The work discussed in this paper extends the methods described to mechanical shock and spherical bend testing, and it also documents improvements to the test setup and data analysis. These improvements include better accuracy in determining the damage location on the printed circuit assembly and enhanced data analysis using absolute energy to identify crack initiation, improving signal to noise. By incorporating these improvements into IPC-9709, best practices will be shared with the industry.

Conclusions

Acoustic emission detection was shown to successfully identify the location of pad craters during spherical bend testing and shock testing. The results were confirmed by dye stain or cross-sectioning. AED has demonstrated improved sensitivity compared to dye stain, and similar sensitivity as cross-sectioning, for identifying pad cratering. A high pass filter is useful to clean data and help identify events of interest. This current state of the art should be incorporated into IPC-9709.

References

[1] Bansal, A New Approach for Early Detection of PCB Pad Cratering Failures, IPC APEX EXPO Proceedings, Las Vegas, NV, 2011.

[2] Bansal, Guirguis, and Liu, Investigation of Pad Cratering in Large Flip-Chip BGA using Acoustic Emission, IPC APEX EXPO Proceedings, San Diego, CA, 2012.

[3] Ralph, Daspit, Cain, Benedetto, Jenkins, Allen, and Newman, Acoustic Emission Detection of BGA Components in Spherical Bend, Proceedings of the Electronic Components and Technology Conference, Las Vegas, NV, pages 208-213, 2013.

[4] Ralph, Daspit, Cain, Benedetto, Jenkins, Allen, and Newman, Acoustic Waveform Energy as an Interconnect Damage Indicator, Conference Proceedings of the Society for Experimental Mechanics, pages 33-42, 2014.

[5] Ralph, Benedetto, Allen, and Newman, Pad Crater Detection Using Acoustic Waveform Analysis, Proceedings of the Electronic Components and Technology Conference, Orlando, FL, pages 1433-1440, 2014.

[6] W. C. Ralph, E. E. Benedetto, G. N. Morscher, K. Newman, M. J. Silk, Detecting Interconnect Damage in Shock Using Acoustic Emission Detection, Proceedings of the 2015 Annual Conference on Experimental and Applied Mechanics, Costa Mesa, CA, June 2015.

[7] Ralph, Morscher, Benedetto, Newman, Silk, Detection of Pad Crater Initiation in Shock Using Acoustic Emission Detection, Proceedings of the Surface Mount Technology Association International Conference, Rosemont, IL, September 2015.

Acoustic Detection of Pad Craters in Mechanical Shock and Transient Bend Tests

Julie Silk[1], Gregory Morscher[2],
Elizabeth Benedetto[3], Douglas Olney[1], W. Carter Ralph[4]

[1]Keysight Technologies,
[2]University of Akron, [3]HP Inc , [4]Southern Research Institute

Agenda

- Pad cratering description and detection
- Acoustic emission background and basics
- Latest developments in data analysis from shock testing
- Spherical bend test setup and results
- Drop/Shock test setup and results
- Comparison of acoustic emission detection with failure analysis
- Conclusions and future work

Pad cratering description

- Pad cratering is a mechanically-induced cohesive failure in the PCB resin layer under a component pad.
- This defect mechanism causes opens in printed circuit assemblies when the crack propagates sufficiently to sever a trace.
- The defect can be latent, causing failure well after the fracture is initiated
- Incidence of pad cratering has increased with stiffer solders and more brittle PCB laminates

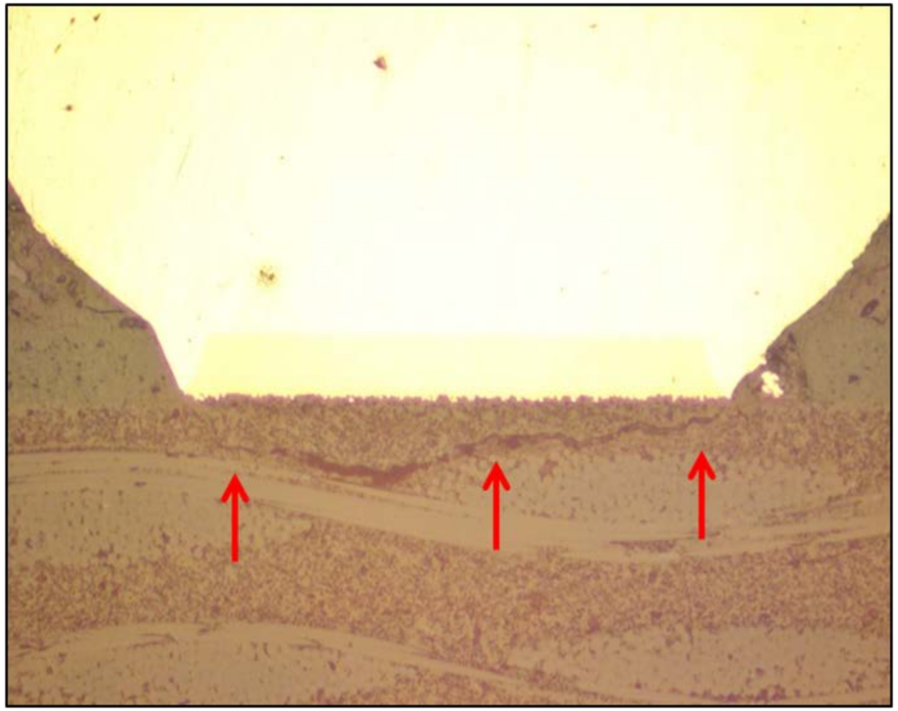

Cross-section showing pad crater under a BGA pad

Pad crater detection

- Electrical monitoring is used in bend and shock tests. Fractures can often occur well in advance of electrical opens.
- Cross-sections and dye stain (dye and pry) of stressed component joints are the typical method of detecting pad craters formed by bend and shock test methods.

Cross-sectioning and dye stain destroy the samples and testing cannot be continued. They are time-consuming and expensive to perform at volumes sufficient to evaluate pad crater risks and to analyze susceptibility of materials and components.

Dye penetration into pad crater

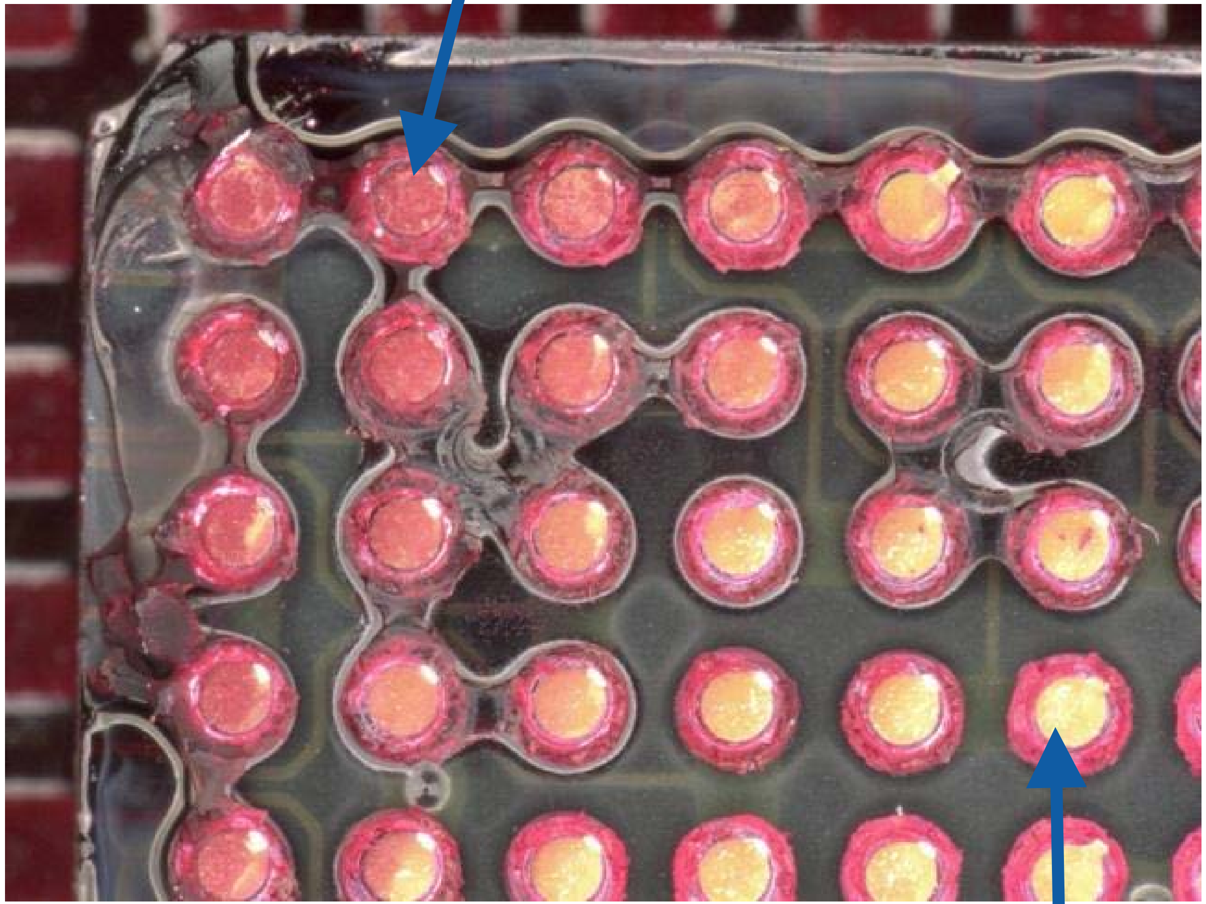

Dye stain showing presence of fractures on BGA balls

No dye penetration

Acoustic Emission

- Acoustic Emission Detection (AED) allows detection of fracture initiation without destroying the samples
- The method was first published in 2011. [1] [2]
- A guideline describing the method and its use with four-point bend testing, IPC- 9709, was introduced in 2013.
- Subsequent work on using AED is presented here:
  - AED during spherical bend testing [3] [4] [5]
  - AED during drop/shock testing [6]
  - Comparison with cross-sections and dye stain [7]
  - Improvements in data analysis techniques

How acoustic emission detection works

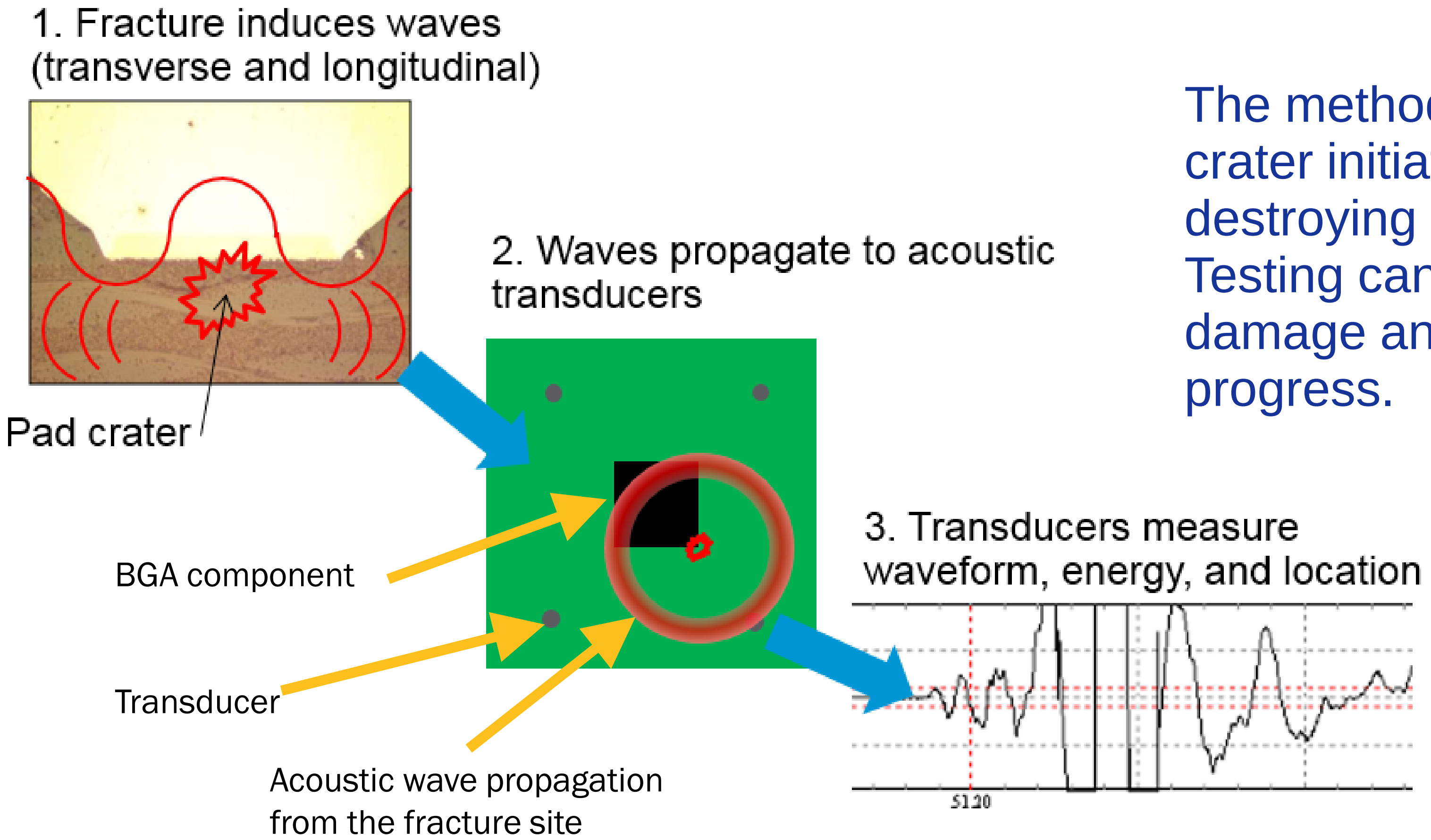

The method can detect pad crater initiation without destroying the sample. Testing can continue as damage and detection progress.

Example of test vehicle with transducers attached

Transducers can be attached with several choices of couplants and attachment methods.

Wide-band transducers used: sensitive to at least 100 kHz and up to 700 kHz, flat frequency response
Test vehicle parameters: 35x35 mm PBGA package, 1 mm pitch SAC305 solder balls, non-solder mask defined pads, 1.6 mm thick, 203x203 mm board

Acoustic emission: locates fracture event

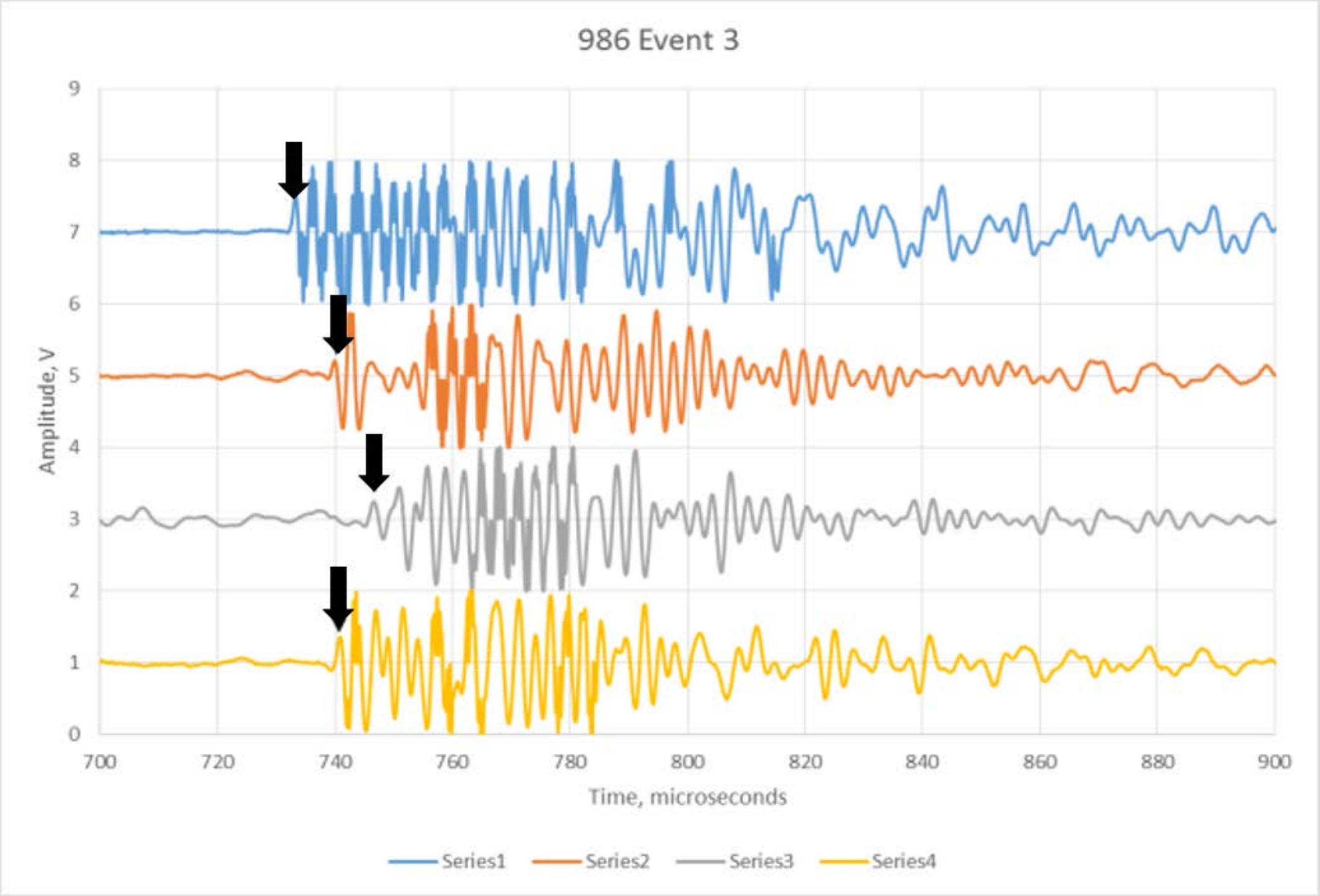

- Acoustic signals travel through the PCB and are detected by transducers

Example of a fracture event with acoustic signal at each of 4 transducers.

The fracture signal, marked by an arrow, arrives at different times for each, allowing the location to be calculated.

AE data processing

- Acoustic data is typically processed using specialized software.
- Pencil lead breaks are used to calculate speed of transmission through the substrate and verify that the sensors are functioning.
- Waveform energy and event location are calculated for each event.
- Acoustic events that are not of interest, such as those not within the board area and those well outside the surface mount component boundary, are eliminated.
- Currently some event detection steps are done manually.

Acoustic signals are complex

- Shown: acoustic signals for a shock/drop event, with magnitude and frequency over time.
- An initial large burst of noise is from the board, fixture and tooling striking the shock equipment.
- This is followed by flexure of the board and associated acoustic noise from mounting points, board and components – including higher energy events from fractures in the laminate

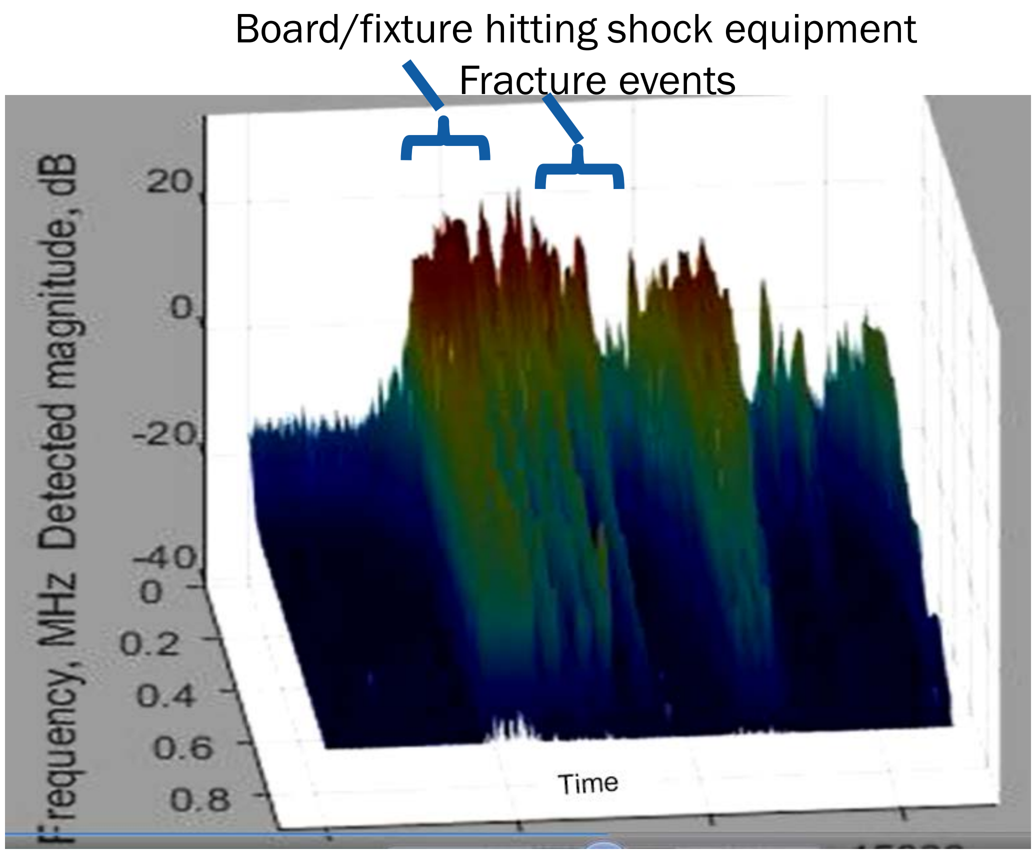

Acoustic Signals in 3D

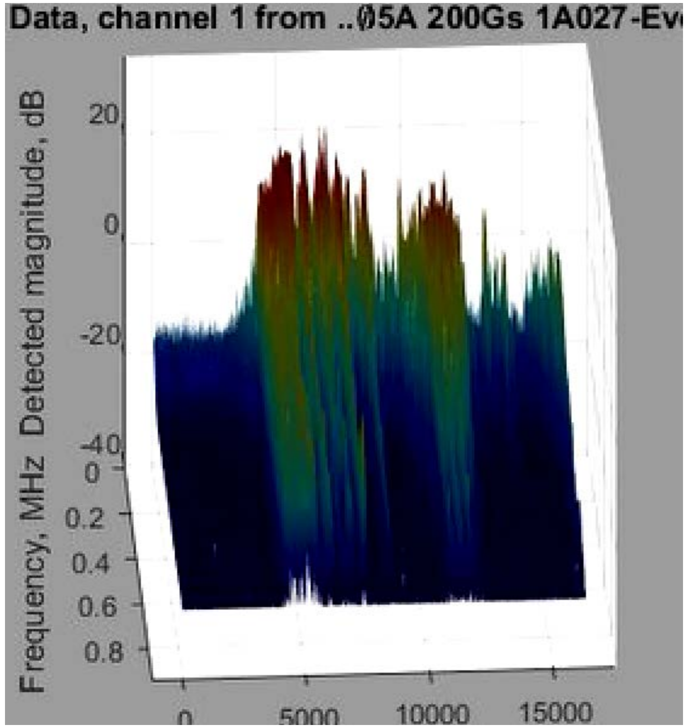

Magnitude vs time

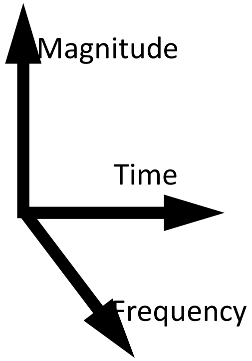

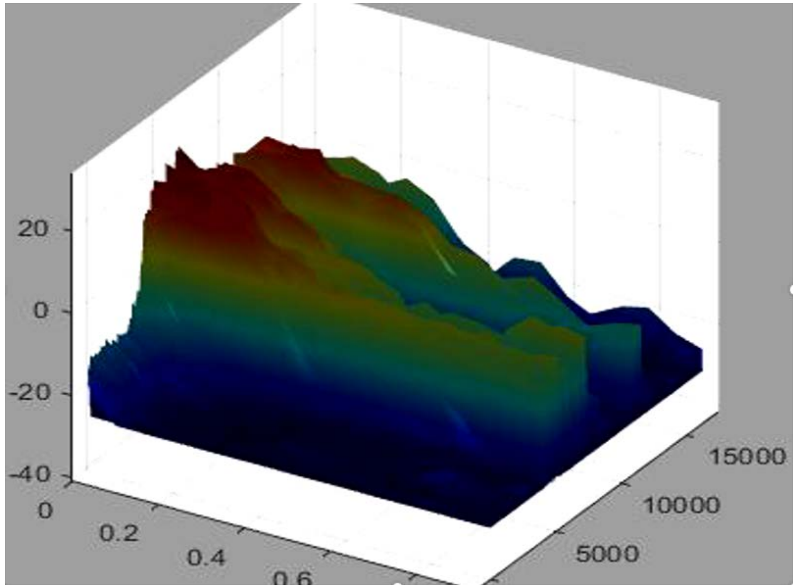

Magnitude vs frequency at beginning of shock event

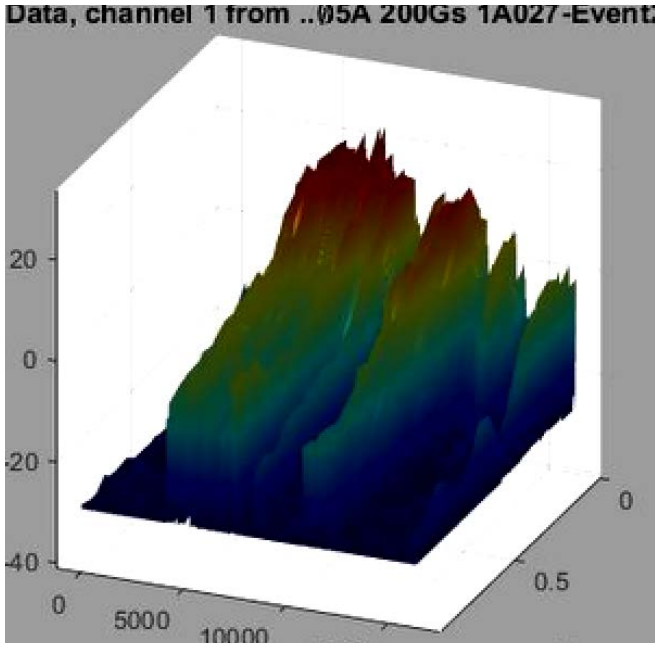

View from later end of shock data

Acoustic emission data analysis

- An appropriate high pass filter can eliminate much of the noise and allow better identification of fracture events.

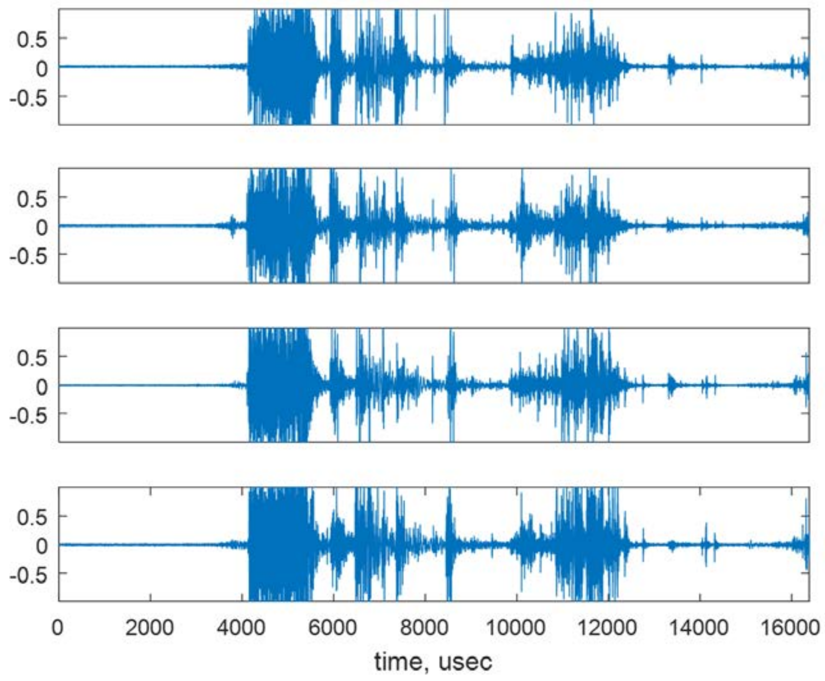

Raw signal

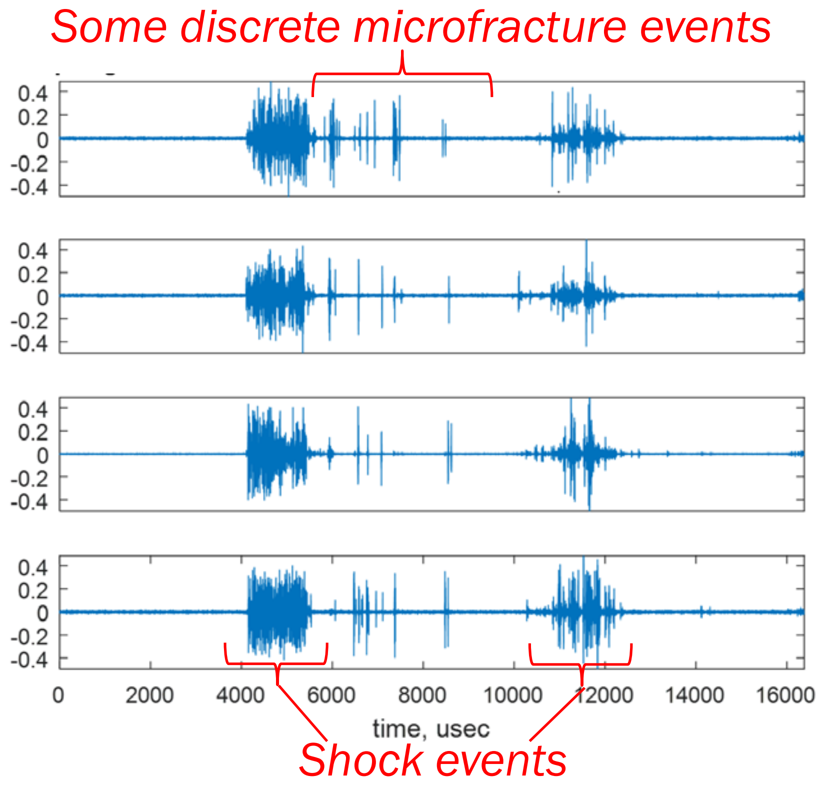

After high pass filter

Spherical Bend Test Vehicle and Setup

- Spherical bend is an alternative to four-point bend testing.
- Spherical bend, being more aggressive, represents the worst case in flexure

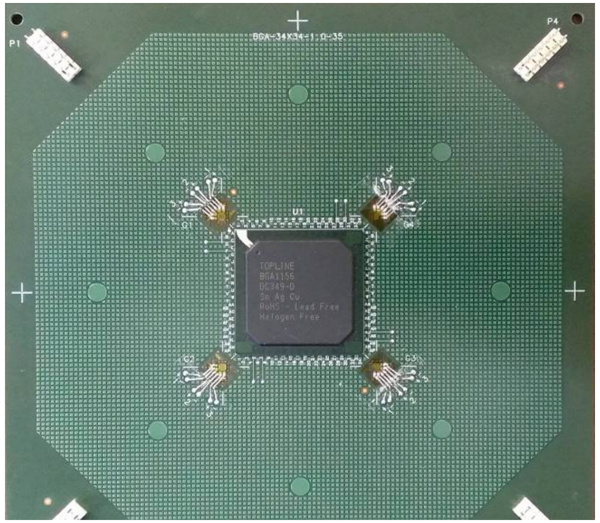

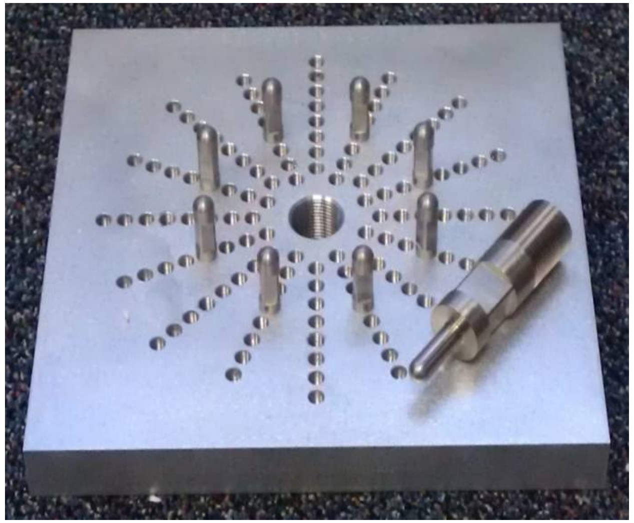

Wide-band transducers, sensitive to at least 100 kHz and up to 700 kHz, flat frequency response
Test vehicle parameters: 35x35 mm PBGA package, 1 mm pitch SAC305 solder balls, non-solder mask defined pads, 1.6 mm thick, 203x203 mm board

Spherical Bend: Event Energy on Component Map

- Transducers - black circles
- Supports - white circles
- Events colored according to time of occurrence, sized according to effective energy
- AED shows events before and after the daisy chain opens – unlike electrical testing

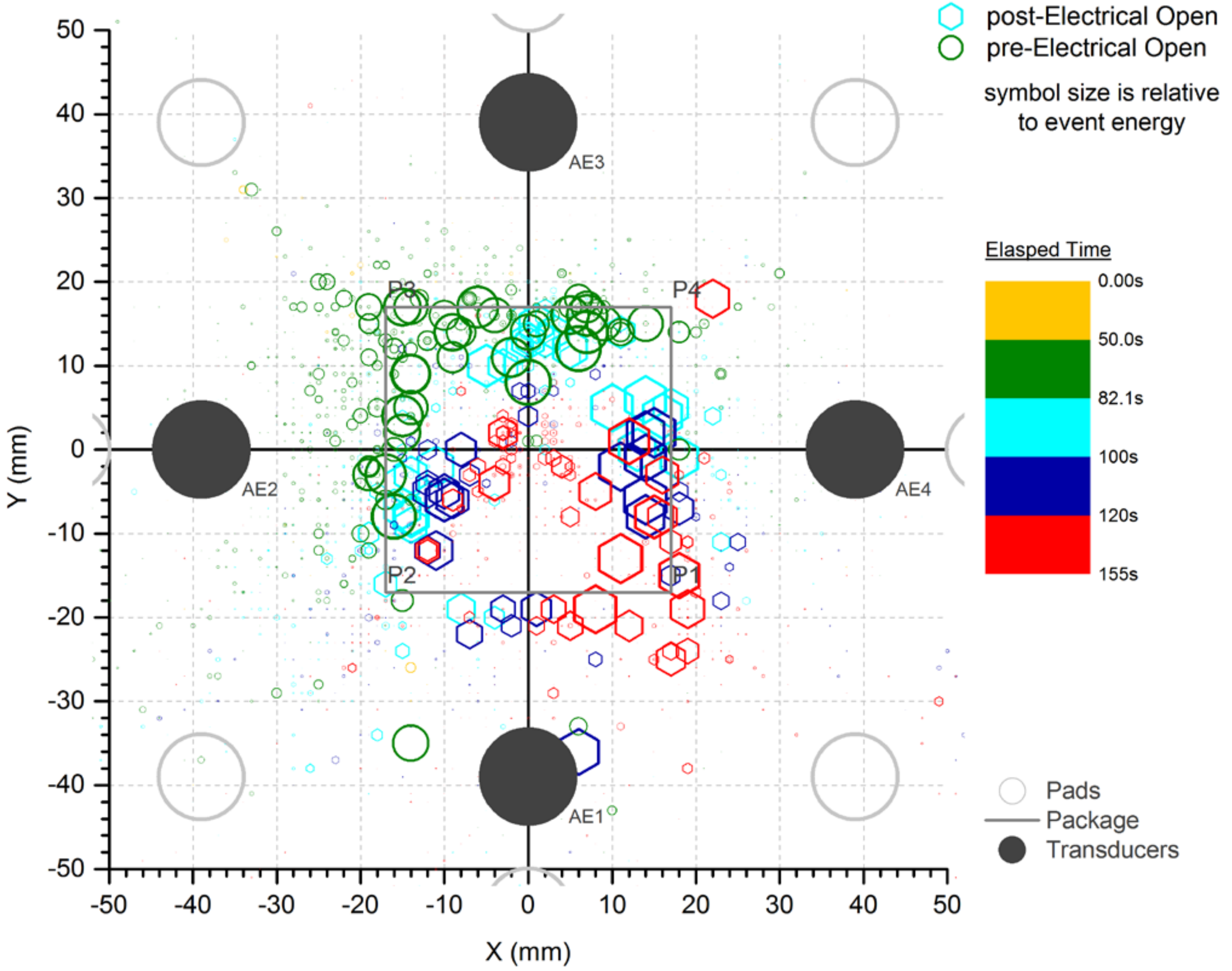

Cumulative energy over time

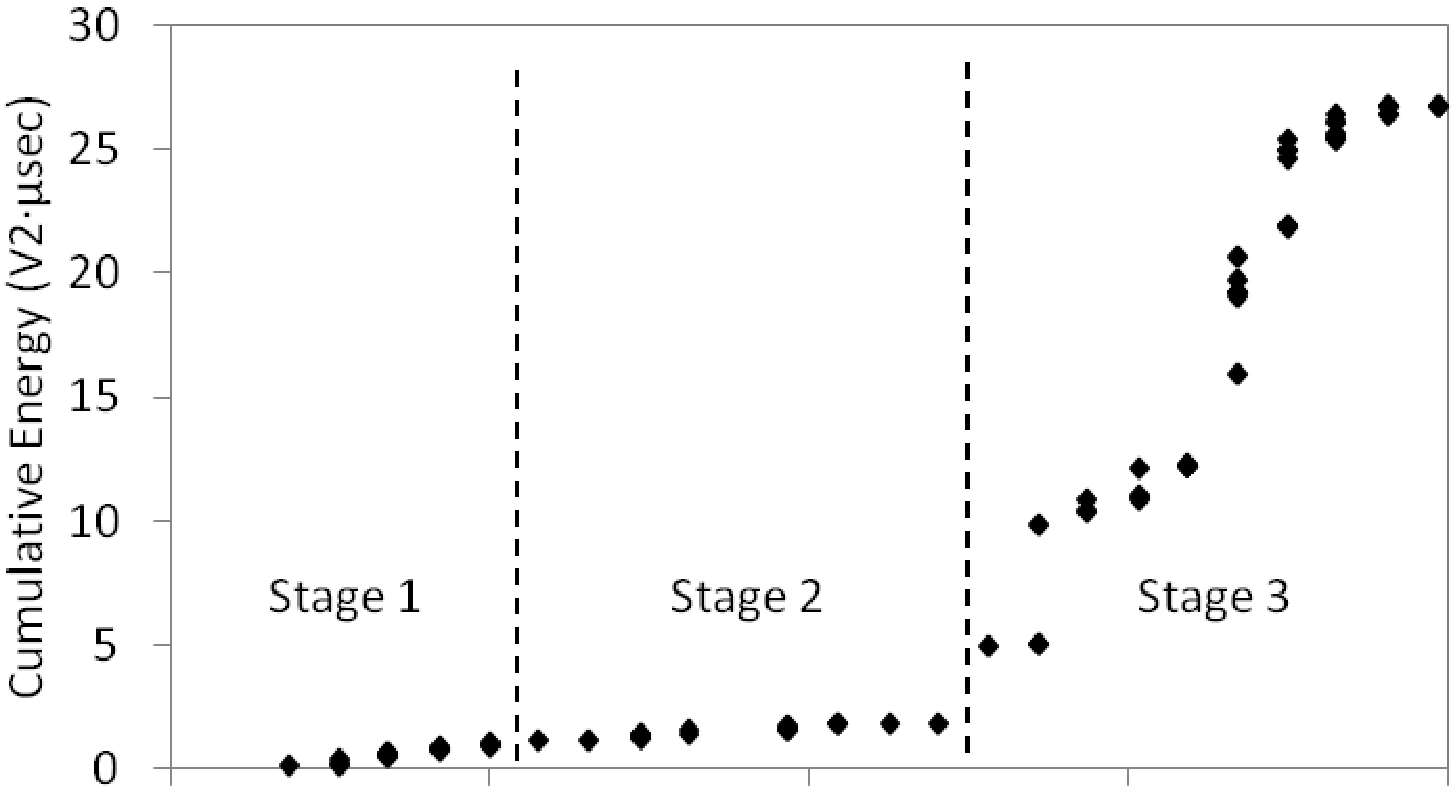

- The acoustic events produced in Stages 1 and 2 are scattered throughout the PCA, such as small-scale damage in the PCA, such as fiber-matrix debonding
- Events in Stage 3 were located within the perimeter of the PBGA, attributed to pad craters

Shock Test Setup

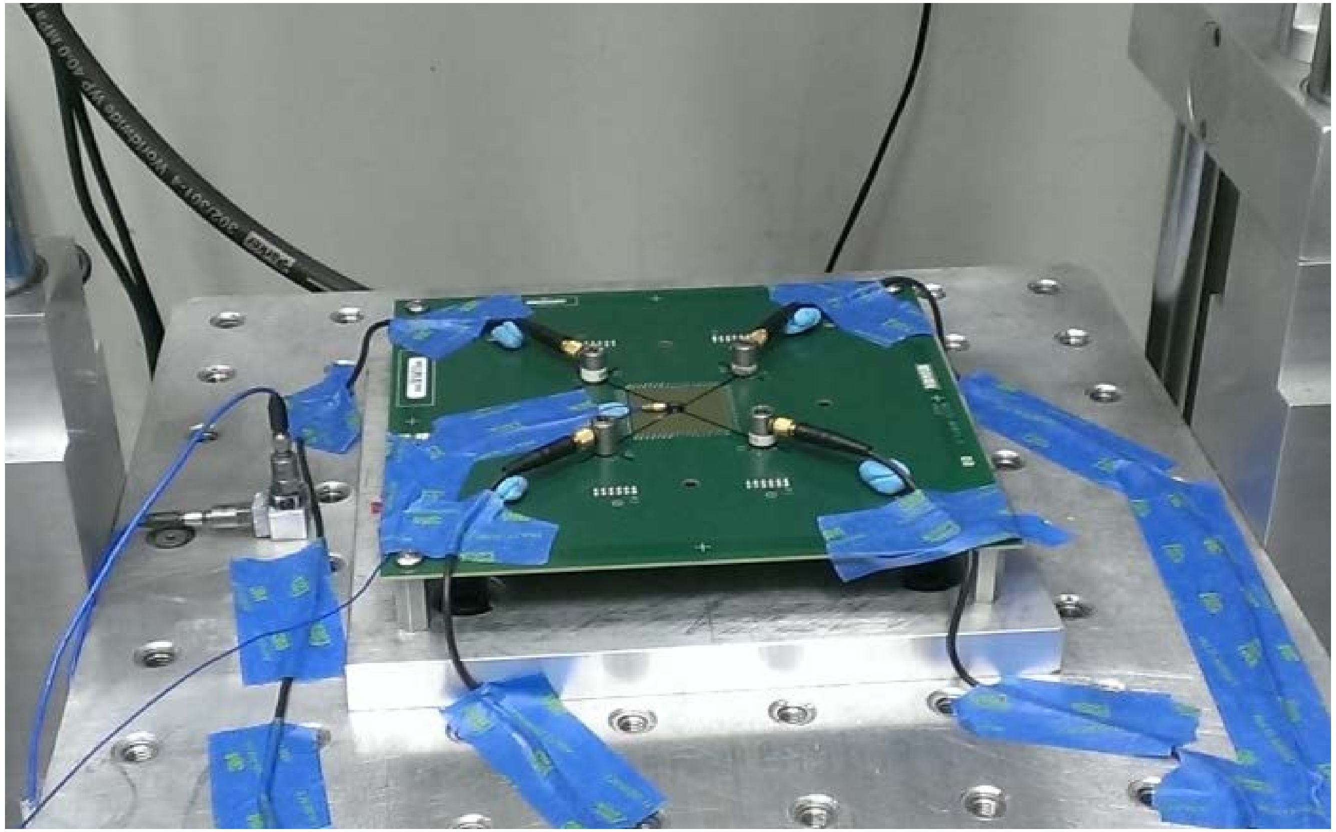

- The same test vehicle was used as for transient bend
- The component is loaded face-down
- Wires are taped to prevent additional noise from wire slapping

Wide-band transducers, sensitive to at least 100 kHz and up to 700 kHz, flat frequency response
Test vehicle parameters: 35x35 mm PBGA package, 1 mm pitch SAC305 solder balls, non-solder mask defined pads, 1.6 mm thick, 203x203 mm board

Comparison of AE with Failure Analysis

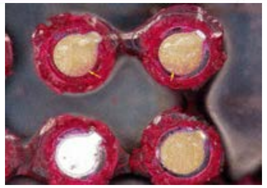

- AE events were confirmed with cross-sections.
- AE detected slightly more damage at lower shock levels than detected by cross-section. A cross-section can miss small areas of damage.
- Dye stain (dye and pry) detected lower or no damage at shock levels where damage was detected with other methods. We suspect that dye could not penetrate when fractures did not reach the surface.

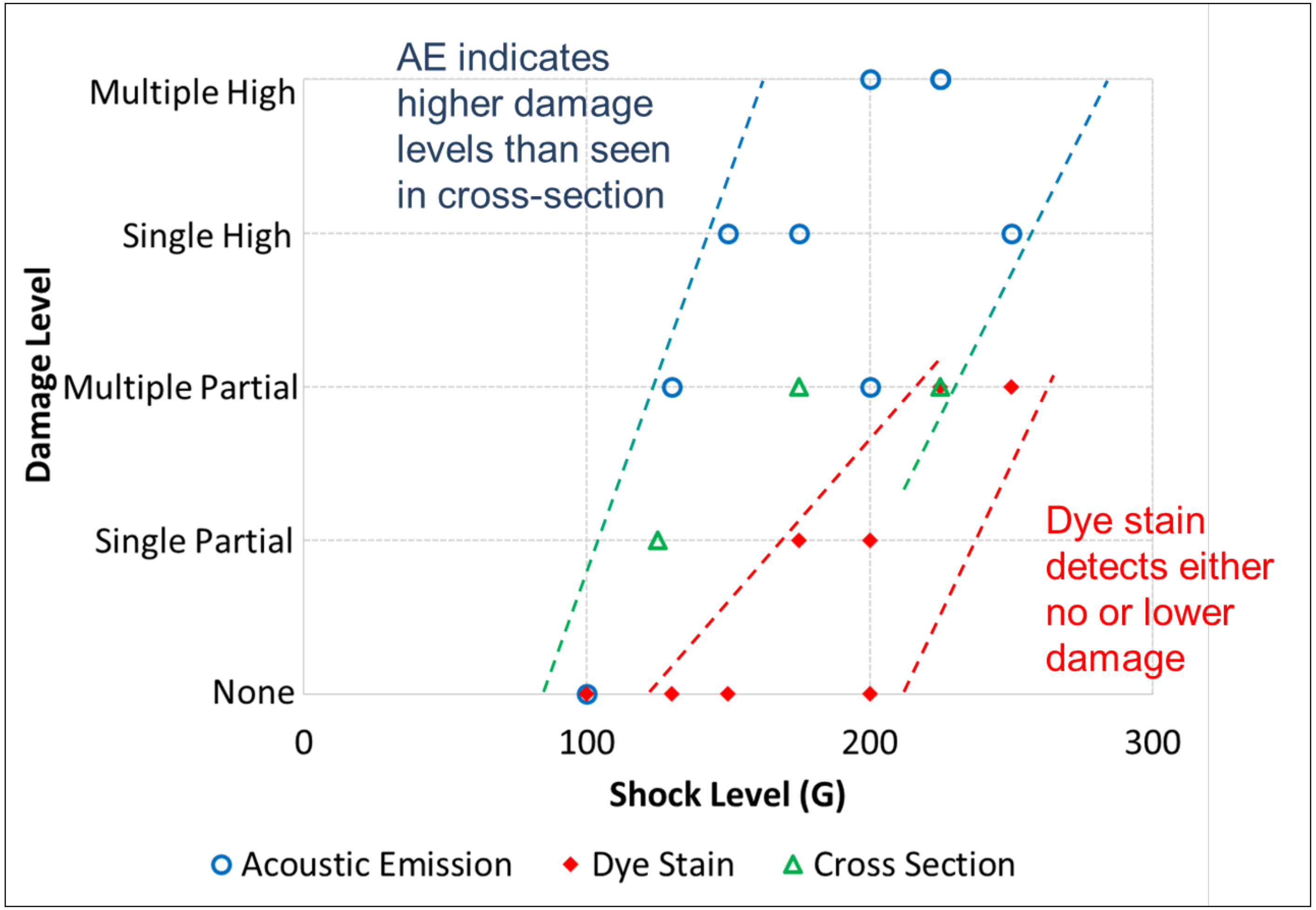

Conclusions

- AE can detect pad crater initiation in both transient bend and shock stresses without destructive analysis
- AE has demonstrated improved sensitivity compared to dye stain for identifying pad cratering
- AE has demonstrated similar sensitivity to cross-sectioning in identifying pad cratering
- High pass filter is useful to clean data and help identify “events of interest”
- Current state of the art needs to be incorporated into IPC 9709

Further work

- The initial publication of IPC 9709 included basic guidelines for use of AED with four-point bend testing. The learnings from this work can be added to enhance this document:
  - Spherical bend
  - Shock/drop
  - Process improvements
  - Improved location accuracy
  - Enhanced data analysis

Acknowledgements to the main experimenters and co-authors :

- Elizabeth Benedetto at HP Inc
- Carter Ralph at Southern Research Institute
- Gregory Morscher at University of Akron

Thank you!

Questions?

Julie Silk, julie_silk@keysight.com

References

[1] Bansal, A New Approach for Early Detection of PCB Pad Cratering Failures, IPC APEX EXPO Proceedings, Las Vegas, NV, 2011.

[2] Bansal, Guirguis, and Liu, Investigation of Pad Cratering in Large Flip-Chip BGA using Acoustic Emission, IPC APEX EXPO Proceedings, San Diego, CA, 2012.

[3] Ralph, Daspit, Cain, Benedetto, Jenkins, Allen, and Newman, Acoustic Emission Detection of BGA Components in Spherical Bend, Proceedings of the Electronic Components and Technology Conference, Las Vegas, NV, pages 208-213, 2013.

[4] Ralph, Daspit, Cain, Benedetto, Jenkins, Allen, and Newman, Acoustic Waveform Energy as an Interconnect Damage Indicator, Conference Proceedings of the Society for Experimental Mechanics, pages 33-42, 2014.

[5] Ralph, Benedetto, Allen, and Newman, Pad Crater Detection Using Acoustic Waveform Analysis, Proceedings of the Electronic Components and Technology Conference, Orlando, FL, pages 1433-1440, 2014.

[6] W. C. Ralph, E. E. Benedetto, G. N. Morscher, K. Newman, J. Silk, Detecting Interconnect Damage in Shock Using Acoustic Emission Detection, Proceedings of the 2015 Annual Conference on Experimental and Applied Mechanics, Costa Mesa, CA, June 2015.

[7] Ralph, Morscher, Benedetto, Newman, Silk, Detection of Pad Crater Initiation in Shock Using Acoustic Emission Detection, Proceedings of the Surface Mount Technology Association International Conference, Rosemont, IL, September, 2015.